

ATP-mediated Ca^{2+} signaling in preglomerular smooth muscle cells

EDWARD W. INSCHO, ALAN C. SCHROEDER, PAUL C. DEICHMANN, AND JOHN D. IMIG
Department of Physiology, Tulane University School of Medicine, New Orleans, Louisiana 70112

Inscho, Edward W., Alan C. Schroeder, Paul C. Deichmann, and John D. Imig. ATP-mediated Ca^{2+} signaling in preglomerular smooth muscle cells. *Am. J. Physiol. 276 (Renal Physiol. 45): F450–F456, 1999.*—We performed studies to determine the effect of extracellular ATP on the intracellular Ca^{2+} concentration ($[\text{Ca}^{2+}]_i$) in freshly isolated microvascular smooth muscle cells (MVSMC). Suspensions of preglomerular MVSMC were prepared by enzymatic digestion and loaded with fura 2. Single cells were studied using a microscope-based fluorescence spectrophotometer during superfusion of a physiological salt solution with 1.8 mM Ca^{2+} and during exposure to similar solutions containing ATP. Under control conditions, baseline $[\text{Ca}^{2+}]_i$ averaged 107 ± 6 nM ($n = 86$ cells from 34 animals). ATP administration elicited concentration-dependent increases in $[\text{Ca}^{2+}]_i$. Exposure to ATP concentrations of 1, 10, and 100 μM increased intracellular Ca^{2+} to peak concentrations of 133 ± 20 , 338 ± 37 , and 367 ± 35 nM, respectively ($P < 0.05$ vs. respective baseline). Steady-state $[\text{Ca}^{2+}]_i$ increased to 113 ± 15 , 150 ± 16 ($P < 0.05$ vs. baseline), and 180 ± 12 nM ($P < 0.05$ vs. baseline) for the same groups. The $[\text{Ca}^{2+}]_i$ response to ATP was also assessed in the absence of extracellular Ca^{2+} and during blockade of L-type Ca^{2+} channels with diltiazem. In these studies, exposure to 100 μM ATP induced a transient peak increase in $[\text{Ca}^{2+}]_i$ with the plateau phase being totally abolished under Ca^{2+} -free conditions and markedly attenuated during Ca^{2+} channel blockade, respectively. These data indicate that ATP-mediated P2-receptor activation increases $[\text{Ca}^{2+}]_i$ in freshly isolated preglomerular MVSMC by stimulating Ca^{2+} release from intracellular stores, in addition to stimulating the influx of extracellular Ca^{2+} through voltage-gated L-type Ca^{2+} channels.

afferent arterioles; calcium channels; cytosolic calcium; diltiazem; renal microcirculation; purinoceptors; calcium release

REGULATION OF renal vascular resistance occurs through a multitude of mechanisms (26). Changes in intrarenal microvascular resistance can be evoked by alterations in perfusion pressure, changes in circulating or locally generated vasoactive agonists, or alterations in intrarenal neural activity. In the kidney, afferent arteriolar resistance accounts for the majority of the preglomerular resistance, and Ca^{2+} plays a major role in the regulation of afferent arteriolar caliber (26). Studies have shown that afferent arteriolar responses to vasoconstrictors involve the activation of L-type Ca^{2+} channels and can be blocked by Ca^{2+} channel antagonists (5, 6, 14, 24, 26). Similarly, preglomerular autoregulatory responses also rely heavily on the activation of L-type Ca^{2+} channels (6, 25, 26). More recently, it has been

shown that Ca^{2+} mobilization from intracellular stores represents an important component of both the afferent and efferent arteriolar response to angiotensin II and norepinephrine and to the preglomerular response to increases in perfusion pressure (16, 31). In studies using isolated arteriolar segments, it has been shown that administration of vasoconstrictors such as angiotensin II, norepinephrine, or endothelin stimulates an increase in intracellular Ca^{2+} (4, 6, 8, 34); however, whether or not those increases in intracellular Ca^{2+} arise from vascular smooth muscle cells, endothelial cells, or both cell types remains uncertain.

Recent studies have centered on the role of adenosine nucleotide-sensitive P2 receptors in the regulation of renal microvascular resistance (17, 18, 20, 35). Those studies have revealed that extracellular ATP increases renal vascular resistance by stimulating a rapid transient vasoconstriction of arcuate and interlobular arteries and sustained vasoconstriction of afferent arterioles (17, 20, 35). Remarkably, ATP does not influence the diameter of efferent arterioles (21). The most pronounced vasoconstriction is observed from afferent arterioles. This response involves activation of Ca^{2+} influx pathways, including activation of L-type Ca^{2+} channels (20, 21). Functional evidence suggests that ATP-mediated afferent arteriolar vasoconstriction is dependent on Ca^{2+} influx (20); however, other studies, using other vascular smooth muscles, have shown that ATP stimulates Ca^{2+} mobilization (15, 22, 27, 30, 32).

The current studies were performed to directly determine the response of preglomerular microvascular smooth muscle cells (MVSMC) to extracellular ATP. Experiments were performed using rat preglomerular smooth muscle cells freshly isolated from interlobular arteries and afferent arterioles. This approach obviated concerns related to cell culture-induced transformation and ensured that the responses observed reflect the responsiveness of cells in the undispersed tissue. Experiments focused on determining the effect of ATP on $[\text{Ca}^{2+}]_i$ and the relative contribution of Ca^{2+} influx versus Ca^{2+} mobilization. Additional studies were performed to determine the role of L-type Ca^{2+} channel activation on the ATP-mediated increase in $[\text{Ca}^{2+}]_i$.

METHODS

Tissue preparation and renal MVSMC isolation. Studies were performed in accordance with the guidelines and practices put forth by the Tulane University Advisory Committee for Animal Resources. Suspensions of preglomerular MVSMC were prepared as previously described (19). Male Sprague-Dawley rats ($n = 40$; 250–375 g) were anesthetized with pentobarbital sodium (40 mg/kg iv), and the abdominal aorta was cannulated via the superior mesenteric artery. The kidneys were flushed with an ice-cold, low- Ca^{2+} physiological salt solution (PSS; 125 mM NaCl, 5.0 mM KCl, 1.0 mM

The costs of publication of this article were defrayed in part by the payment of page charges. The article must therefore be hereby marked "advertisement" in accordance with 18 U.S.C. Section 1734 solely to indicate this fact.

MgCl_2 , 10 mM glucose, 20 mM HEPES, 0.1 mM CaCl_2 , and 0.1 g/l BSA) before being perfused with a similar solution containing iron oxide (25 mg/ml). All solutions were prepared using highly purified water deionized by a Milli-Q_{PLUS} reverse-osmosis water purification system (Millipore, Bedford, MA).

The kidneys were resected from the animal and decapsulated, and the renal medullary tissue was removed. The cortical tissue was pressed through a 180- μm -mesh sieve, and the sieve retentate was washed several times with ice-cold, low- Ca^{2+} PSS. The vascular tissue remaining on the sieve was transferred to a dish containing ice-cold, low- Ca^{2+} PSS, where segments of interlobular artery with attached afferent arterioles were collected and transferred to a 25-ml dissociation flask containing an enzyme solution of the following composition: 0.15% collagenase (type IV; Sigma Chemical, St. Louis, MO), 0.006% elastase (type II-A; Sigma Chemical), 0.05% soybean trypsin inhibitor (type I-S; Sigma Chemical), and 0.05% BSA dissolved in low- Ca^{2+} PSS. The tissue was incubated in the enzyme solution for 20 min at 37°C before being gently triturated with a pasteur pipette. The vascular segments containing iron oxide were collected with a magnet while the nonvascular tissue cellular debris was decanted. Fresh enzyme solution was added to the flask, and the tissue was incubated at 37°C for another 20 min. Microvascular segments containing iron were washed for 10 min in an ice-cold, enzyme-free recovery solution of the following composition (in mM): 80.0 KCl, 30.0 KH_2PO_4 , 5.0 MgSO_4 , 20.0 glucose, 5.0 Na_2ATP , 5.0 phosphocreatine, 3.0 EGTA, and 10.0 MOPS, pH 7.3 (12). The tissue was gently triturated and the undispersed tissue was transferred to a new aliquot of fresh buffer. This cycle of trituration and transfer was repeated 4–5 times, after which the remaining tissue was discarded. Trituration fractions containing healthy viable cells were centrifuged at 5,800 *g* for 30 s, and the cell pellet was resuspended in ice-cold medium 199 (Sigma Chemical) containing 100 U/ml penicillin and 200 $\mu\text{g}/\text{ml}$ streptomycin and supplemented with 10% (vol/vol) fetal calf serum (M-199; Whittaker Bioproducts, Walkersville, MD). Cell suspensions were stored on ice and were used 1–6 h after isolation.

Fluorescence measurements in single MVSMC. We performed experiments using a monochromator-based fluorescence spectrophotometer equipped with a 75-W xenon bulb and chopper wheel (Photon Technology International, South Brunswick, NJ) (19). Excitation wavelengths of 340 and 380 nm were delivered to the sample chamber through a fiber-optic cable, and the emitted light was collected at 510 nm (Photon Technology International). Slit widths of 3 nm were set for both excitation monochromators. The optical path included a $\times 40$ objective (Nikon Fluor 40, NA = 1.3; Nikon Instruments, Tokyo, Japan) and a dichroic mirror (DM400; Nikon Instruments). Measurements of fluorescence intensity were collected at five data points per second and were analyzed with the aid of the Photon Technology International software. Calibration of the fluorescence data was accomplished *in vitro* according to the method of Gryniewicz et al. (13). The ratio (*R*) of fura 2 fluorescence emitted by 340- and 380-nm (340/380) excitation wavelengths provides an index of the $[\text{Ca}^{2+}]_i$ in these cells. The minimum *R* (R_{\min}) calibration solution contained 1.0 μM fura 2 pentapotassium salt in a solution of (in mM) 115.0 KCl, 20.0 NaCl, 10.0 MOPS, 1.1 MgCl_2 , and 10.0 EGTA, with the pH adjusted to 7.05. The maximum *R* (R_{\max}) solution was identical to the R_{\min} solution except that saturating CaCl_2 was added to yield a free Ca^{2+} concentration of 1.8 mM. R_{\min} and R_{\max} values obtained from this calibration averaged 0.46 ± 0.01 and 16.77 ± 2.47 , respectively, and the 380-nm signals obtained in the presence

and absence of saturating Ca^{2+} (S_{12} and S_{b2} , respectively) averaged 12.65 ± 1.66 ($n = 10$).

For determination of $[\text{Ca}^{2+}]_i$, suspensions of freshly isolated renal microvascular cells were loaded with the Ca^{2+} -sensitive fluorescent probe fura 2-AM (Molecular Probes, Eugene, OR). The cells were loaded at room temperature with 4.0 μM fura 2-AM for 45 min. An aliquot of cell suspension was transferred to the perfusion chamber (Warner Instrument, Hamden, CT), and the cells were allowed to adhere for ~ 30 min. The perfusion chamber was mounted to the stage of a Nikon Diaphot inverted microscope and was attached to a peristaltic perfusion pump. The cells were continuously superfused at room temperature (900 $\mu\text{l}/\text{min}$) with a normal Ca^{2+} PSS solution of the following composition (in mM): 125 NaCl, 5.0 KCl, 1.0 MgCl_2 , 10.0 glucose, 20.0 HEPES, 1.8 CaCl_2 , and 0.1 g/l BSA. Selected cells were isolated in the adjustable sampling window, excluding adjacent cells and/or debris from the sampling field. All fluorescence measurements were obtained with background subtraction.

We determined the effect of ATP on cytosolic Ca^{2+} concentration by exposing single cells to normal- Ca^{2+} PSS solutions containing ATP concentrations of 1, 10, or 100 μM . Other studies were performed to determine the role of extracellular Ca^{2+} on the increase in cytosolic Ca^{2+} induced by ATP. Cells were superfused with a nominally Ca^{2+} -free solution (Ca^{2+} -free PSS), which resembled the PSS solutions except that no CaCl_2 was added. No EGTA was added to the solution, as this may have had a deleterious effect on the ability of the cells to stably regulate resting cytosolic Ca^{2+} concentration. Previous studies have shown that exposure of conglomerular MVSMC to 90 mM KCl in a similar nominally Ca^{2+} -free solution resulted in no detectable increase in cytosolic Ca^{2+} (19). The role of L-type Ca^{2+} channels in the ATP-mediated Ca^{2+} response was assessed by adding 10 μM diltiazem to a normal PSS solution containing 1.8 mM Ca^{2+} .

Statistical analysis. Data are presented as representative traces or as grouped data. Grouped data are presented as the group mean \pm SE. Differences within groups were analyzed by analysis of variance for repeated measures. Differences between groups were analyzed by one-way analysis of variance. Post hoc tests were performed using the Newman-Keuls multiple-range test. $P < 0.05$ was considered significantly different.

RESULTS

Figure 1 presents photographs obtained from videotaped records of a typical freshly isolated MVSMC before, during, and after exposure to ATP. As can be seen in Fig. 1A, the cell exhibits an appropriate fusiform shape typical of vascular smooth muscle cells. During exposure to ATP (Fig. 1B), the cell responds with a marked and rapid shortening from the slender fusiform shape to a rounder shape consistent with smooth muscle contraction. Under control conditions, this cell measured ~ 41 μm in length and 7 μm in width across the center, and the sarcolemma had a smooth, uniform appearance. This cell is pictured again shortly after exposure to a bathing solution containing 100 μM ATP (Fig. 1B). The cell responded with a rapid contraction that reduced the cell length by $\sim 63\%$ to 15 μm and increased the width to ~ 8 μm . During the contractile response, the sarcolemma could be seen to change from a smooth uniform appearance to a coarse, more contorted appearance, with pronounced indentations and protrusions in the plasma membrane (Fig. 1B). How-

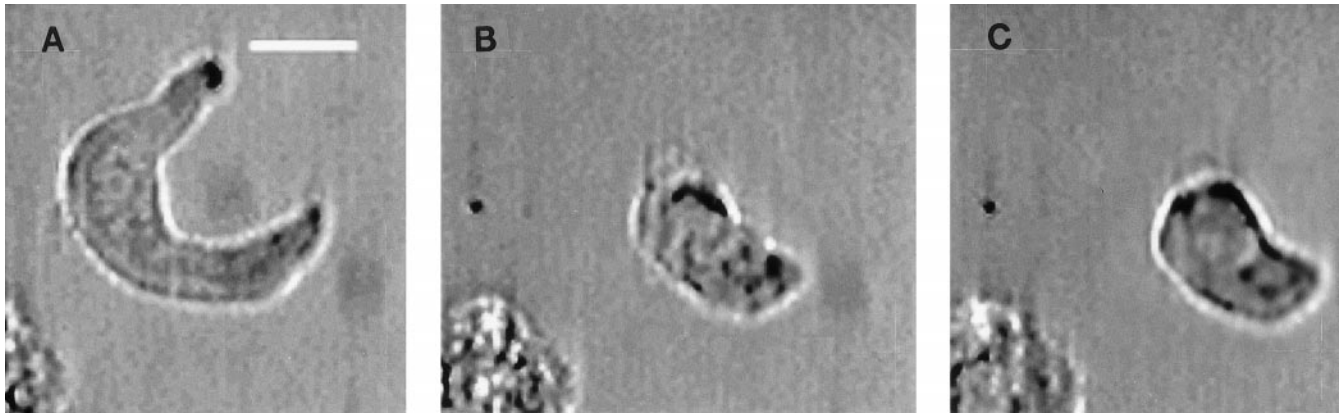


Fig. 1. Photographs of a freshly isolated microvascular smooth muscle cell (MVSMC) before (A), during (B), and after exposure to 100 μ M ATP (C). Photographs of videotaped images were taken at same magnification using digital CCD camera. White bar represents 10 μ m, as determined using stage micrometer.

ever, when the ATP was removed from the bathing medium and the cell was allowed to relax, the undulations of the cell surface disappeared and the sarcolemma reverted to a smoother, more uniform appearance (Fig. 1C).

The first series of experiments was performed to determine the effect of extracellular ATP on $[Ca^{2+}]_i$ in freshly isolated rat renal MVSMC. The results of those studies are presented in Figs. 2 and 3. Experiments were performed using ATP concentrations of 1, 10, and 100 μ M, amounts that have been shown to cause significant vasoconstriction of juxtamedullary afferent arterioles (17). Figure 2 presents a representative trace depicting the $[Ca^{2+}]_i$ response obtained at each of the three ATP concentrations tested. As shown in Fig. 2, ATP caused a rapid and concentration-dependent increase in $[Ca^{2+}]_i$ that was completely reversible. The biphasic increase in $[Ca^{2+}]_i$ typically included a rapid initial increase to a peak value followed by a partial recovery to a plateau concentration. Removal of ATP from the superfusion solution resulted in a rapid return of the $[Ca^{2+}]_i$ to a concentration similar to the control value.

Figure 3 illustrates the average data obtained from multiple cells and tissue dispersions. Resting $[Ca^{2+}]_i$ averaged 107 nM ($n = 86$ cells from 34 animals). Extracellular ATP concentrations of 1, 5, 10, and 100

μ M evoked significant peak increases in $[Ca^{2+}]_i$ to 133 ± 20 , 230 ± 57 , 338 ± 37 , and 367 ± 35 nM, respectively. Sustained elevations in $[Ca^{2+}]_i$ were observed with ATP concentrations of 5, 10, and 100 μ M and averaged 111 ± 9 , 150 ± 16 , and 180 ± 12 nM, respectively ($P < 0.05$ vs. the resting $[Ca^{2+}]_i$ under control conditions).

We evaluated the role of Ca^{2+} influx in the ATP-induced increase in $[Ca^{2+}]_i$ in single MVSMC. These experiments were performed by exposing single cells to a solution containing 100 μ M ATP in the absence of extracellular Ca^{2+} . A representative example of these experiments is presented in Fig. 4, and the mean data are presented in Fig. 5. As shown in Fig. 4, removal of Ca^{2+} from the extracellular medium resulted in a slight drop in $[Ca^{2+}]_i$ from ~ 57 nM to ~ 40 nM, at which point it stabilized. Administration of 100 μ M ATP in the absence of extracellular Ca^{2+} resulted in a sharp rise in $[Ca^{2+}]_i$ that peaked rapidly before quickly returning to a value near baseline. Figure 5 presents the average data obtained from 15 cells from 10 different dispersions. These data are compared with the responses obtained from control cells (Fig. 2) receiving 100 μ M ATP in the presence of 1.8 mM of extracellular Ca^{2+} . In the control group of cells, 100 μ M ATP increased $[Ca^{2+}]_i$ by 254 ± 34 nM to a peak value of 367 ± 35 nM before returning to the plateau $[Ca^{2+}]_i$ of 180 ± 12 nM. This

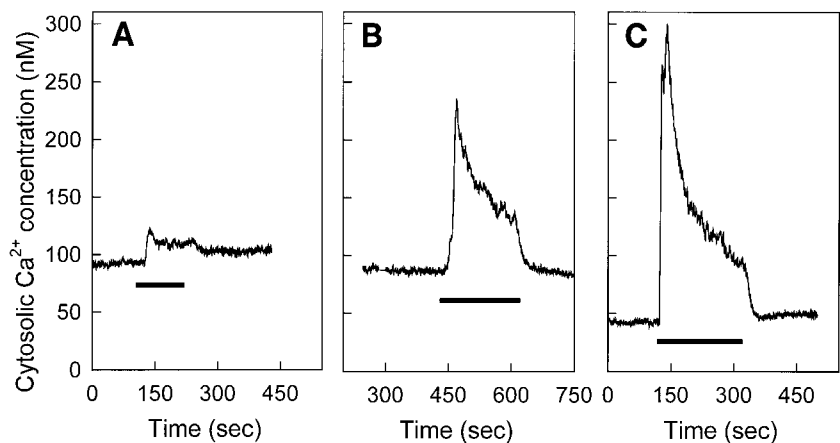


Fig. 2. Effect of increasing ATP concentration on intracellular Ca^{2+} ($[Ca^{2+}]_i$) concentration in MVSMC. Characteristic responses are illustrated in 3 typical traces depicting response of different cells to ATP concentrations of 1, 10, and 100 μ M (A–C, respectively).

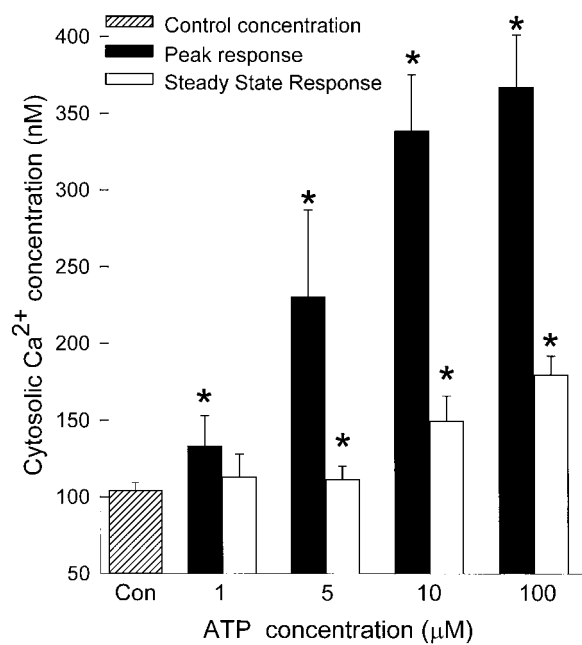


Fig. 3. Effect of increasing ATP concentration on $[\text{Ca}^{2+}]_i$ of renal MVSMC. Data represent average responses obtained from minimum of 8 cells from 4 dissociations for each ATP concentration tested. *Significant increase in Ca^{2+} over baseline.

plateau $[\text{Ca}^{2+}]_i$ is 67 ± 9 nM higher than the baseline $[\text{Ca}^{2+}]_i$. The cells to be exposed to Ca^{2+} -free conditions had a baseline Ca^{2+} concentration of 72 ± 7 nM; this $[\text{Ca}^{2+}]_i$ decreased by 19 nM, to 53 ± 4 nM, in the absence of extracellular Ca^{2+} . Exposure to 100 μM ATP, in the absence of extracellular Ca^{2+} , resulted in a rapid increase in $[\text{Ca}^{2+}]_i$ of 117 ± 33 nM, to a peak value of 169 ± 33 nM, before returning to a sustained $[\text{Ca}^{2+}]_i$ of 48 ± 4 nM. The magnitude of the peak response to 100 μM ATP was reduced by $\sim 50\%$ in the absence of extracellular Ca^{2+} compared with cells stimulated in

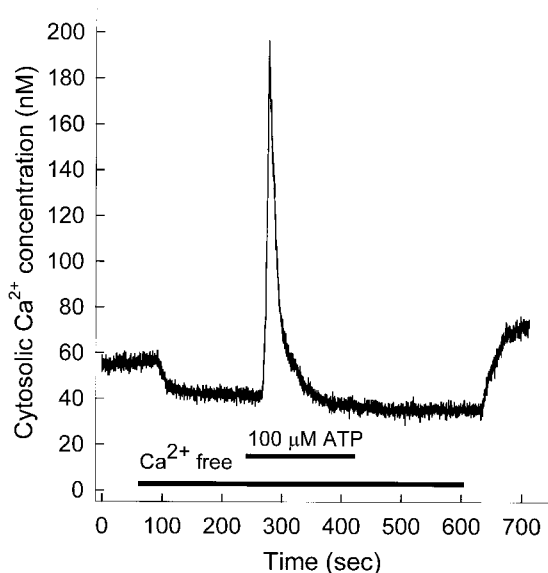


Fig. 4. Response of renal MVSMC to ATP in absence of extracellular Ca^{2+} . Exposure to Ca^{2+} -free medium and to combination of 100 μM ATP in Ca^{2+} -free medium are depicted by solid lines.

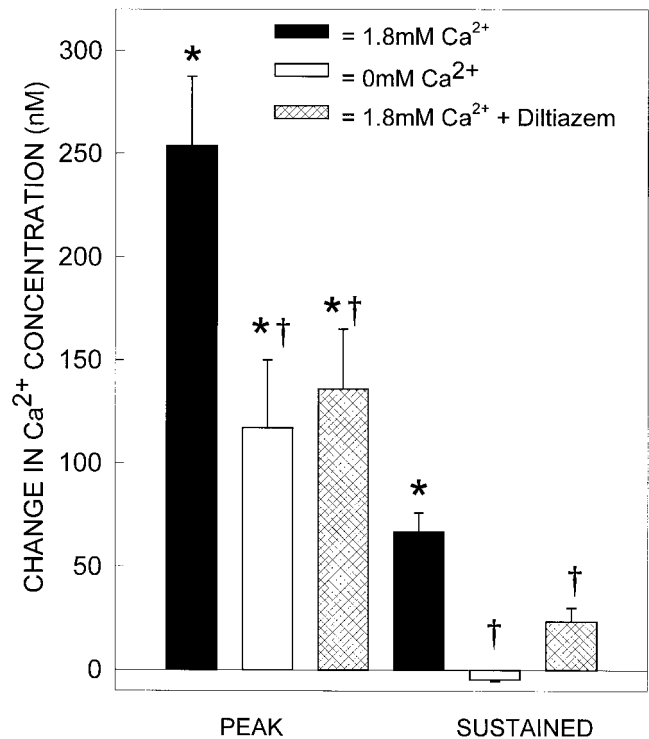


Fig. 5. Average effect of 100 μM ATP on peak and sustained changes in $[\text{Ca}^{2+}]_i$ of renal MVSMC in presence of 1.8 mM extracellular Ca^{2+} ($n = 52$ cells from 26 dissociations), Ca^{2+} -free bathing solution ($n = 15$ cells from 10 dissociations), and 1.8 mM extracellular Ca^{2+} + 10 μM diltiazem ($n = 15$ cells from 4 dissociations). *Significant increase in Ca^{2+} over baseline; †significant difference compared with response in 1.8 mM Ca^{2+} alone.

the presence of 1.8 mM Ca^{2+} (Fig. 2). The plateau phase was completely abolished during exposure to Ca^{2+} -free bathing medium. Similar results were obtained in experiments in which 0.125 mM EGTA was added to the nominally Ca^{2+} -free medium (data not shown).

The afferent arteriolar vasoconstrictor response induced by ATP has been shown to involve activation of voltage-gated L-type Ca^{2+} channels (20). Therefore, we determined the effect of blocking voltage-dependent Ca^{2+} influx with diltiazem, a selective antagonist of L-type Ca^{2+} channels. The representative trace provided in Fig. 6 demonstrates that preincubation with 10 μM diltiazem did not significantly alter the resting $[\text{Ca}^{2+}]_i$; however, it did reduce the peak and plateau increase in $[\text{Ca}^{2+}]_i$ induced by subsequent exposure to 100 μM ATP in the continued presence of 10 μM diltiazem. The mean responses obtained from multiple cells are summarized in Fig. 5. Under control conditions, resting $[\text{Ca}^{2+}]_i$ averaged 111 ± 9 nM. Exposure of the cells to 10 μM diltiazem did not alter $[\text{Ca}^{2+}]_i$ (110 ± 9 nM) and, on exposure to 100 μM ATP, $[\text{Ca}^{2+}]_i$ increased significantly by 136 ± 29 nM to a peak $[\text{Ca}^{2+}]_i$ of 246 ± 31 nM. The peak response quickly waned until it reached a plateau $[\text{Ca}^{2+}]_i$ of 133 ± 9 nM, which is only 24 ± 7 nM higher than the baseline $[\text{Ca}^{2+}]_i$. Both the peak and the sustained elevation of $[\text{Ca}^{2+}]_i$ induced by extracellular ATP were significantly attenuated by $\sim 50\%$ in the presence of diltiazem.

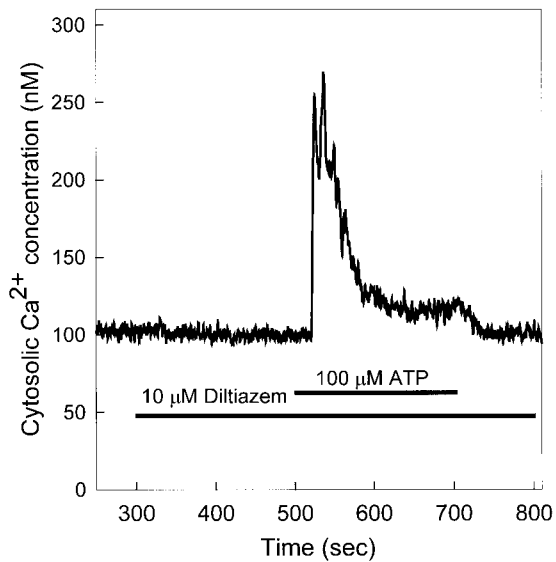


Fig. 6. Effect of blockade of voltage-gated Ca^{2+} channels on increase in $[\text{Ca}^{2+}]_i$ elicited by $100 \mu\text{M}$ ATP with 1.8 mM Ca^{2+} in bathing solution. Trace is representative of several experiments and depicts effect of diltiazem, alone and in combination with $100 \mu\text{M}$ ATP, on cytosolic Ca^{2+} concentration. Exposure to diltiazem and exposure to diltiazem plus ATP are depicted by solid lines.

DISCUSSION

P2 receptors are subdivided into two major receptor families classified as P2X and P2Y (1, 3, 11). Both receptor subtypes appear to be expressed by afferent arterioles (7, 17, 20), and both receptor families appear to elicit cellular responses through activation of Ca^{2+} signaling pathways (1, 9, 20). Therefore the current studies were performed to determine the effect of extracellular ATP on the concentration of Ca^{2+} in the sarcoplasm of smooth muscle cells freshly isolated from the preglomerular microvasculature. The results of these studies demonstrate that ATP stimulates an increase in $[\text{Ca}^{2+}]_i$ through mechanisms that involve both the release of Ca^{2+} from intracellular stores and the influx of Ca^{2+} from the extracellular medium.

Exposure of MVSMC to extracellular ATP results in an increase in $[\text{Ca}^{2+}]_i$ that is dose dependent and rapidly reversible. Although we cannot make direct associations between the Ca^{2+} signaling responses observed in the current report and previous observations describing ATP-mediated preglomerular vasoconstriction, some very interesting similarities are apparent. The kinetics of the Ca^{2+} response are biphasic, beginning with a rapid transient increase that reaches a peak value before quickly declining to a more stable plateau concentration. This Ca^{2+} response pattern is consistent with what has been shown for other vascular smooth muscle cells (2, 15, 33) and closely mimics the vasoconstrictor response that is observed from preglomerular microvascular segments (17, 20). Furthermore, the ATP concentrations found to significantly increase $[\text{Ca}^{2+}]_i$ in MVSMC are identical to the concentrations found to significantly vasoconstrict rat juxtamedullary afferent arterioles (17, 20). Therefore, these data are consistent with the hypothesis that ATP

stimulates afferent arteriolar vasoconstriction by activating P2 receptors on the renal MVSMC and stimulating a rapid increase in $[\text{Ca}^{2+}]_i$.

The dependency of preglomerular vasoconstriction on the activation of voltage-gated L-type Ca^{2+} channels has been established by the work of many investigators (5, 6, 14, 20, 24, 26, 29). Loutzenhiser et al. (23) recently determined that afferent and efferent arterioles of the hydronephrotic kidney perfused at 80 mmHg have resting membrane potentials between -38 and -40 mV, which is near the activation potential for L-type Ca^{2+} channels. Ca^{2+} channel blockade potentially attenuates or abolishes afferent arteriolar responses to a multitude of vasoactive agonists that influence renal microvascular resistance. Interestingly, these Ca^{2+} channel blockers are ineffective at blocking efferent arteriolar responses to the same agonists (5, 8, 24, 26). Exposure of MVSMC to extracellular ATP results in an increase in $[\text{Ca}^{2+}]_i$ that is blunted in the presence of Ca^{2+} channel blockers but not abolished. As shown in Fig. 6, pretreatment with diltiazem reduced the magnitude of the peak increase in $[\text{Ca}^{2+}]_i$ by $\sim 50\%$ and reduced the sustained elevation in $[\text{Ca}^{2+}]_i$ by $\sim 70\%$. Consistent with this observation, we have shown that the Ca^{2+} channel antagonists diltiazem and flodipine markedly attenuated the initial vasoconstriction evoked by the P2X agonist α, β -methylene ATP while abolishing the sustained vasoconstriction (20). Collectively, these observations suggest that activation of voltage-gated L-type Ca^{2+} channels plays a major role in ATP-mediated elevation of $[\text{Ca}^{2+}]_i$ and in ATP-mediated afferent arteriolar vasoconstriction.

It is interesting to note that diltiazem did not completely block the increase in intracellular Ca^{2+} (Figs. 5 and 6) nor did it completely prevent transient ATP-mediated vasoconstriction (20). The explanation for this apparent "diltiazem-insensitive" Ca^{2+} response remains to be determined; however, it appears to be of extracellular origin given that it was not observed under Ca^{2+} -free conditions (Figs. 4 and 5). One possible explanation is that diltiazem is use dependent and that complete blockade of L-type Ca^{2+} channels was not achieved. This could have permitted some Ca^{2+} to enter the cells and could account for the small increase. In a previous report, a similar residual increase was observed in response to KCl depolarization in the presence of diltiazem (19). Importantly, the residual increase in $[\text{Ca}^{2+}]_i$ persisted despite repeated KCl challenges in the continuous presence of diltiazem. Furthermore, neither diltiazem nor flodipine could completely block P2 receptor-mediated afferent arteriolar vasoconstriction, whereas removal of extracellular Ca^{2+} did. The persistence of the response, despite repeated depolarizing stimuli, and the fact that two structurally distinct classes of Ca^{2+} channel blockers did not completely block P2 receptor-mediated vasoconstrictor responses argue against use dependency of diltiazem being a likely explanation for the diltiazem-insensitive increase in $[\text{Ca}^{2+}]_i$. Alternatively, this response could derive from a voltage-dependent pathway that is insensitive to L-type Ca^{2+} channel antagonists.

Gordienko et al. (12) reported that vascular smooth muscle cells isolated from rat arcuate arteries express T-type Ca^{2+} channels, which are reported to be insensitive to L-type Ca^{2+} channel antagonists. Depolarization of the sarcolemma with KCl or ATP would activate T channels and initiate Ca^{2+} influx through a diltiazem- and felodipine-insensitive pathway and thus could explain the increase in $[\text{Ca}^{2+}]_i$ observed in the presence of diltiazem. A third possibility should also be considered. Binding of ATP to P2X receptors is believed to produce vasoconstriction by activating receptor-operated, nonselective cation channels, which are an integral part of the P2X receptor proteins (28). Activation of these ligand-gated channels leads to the influx of Ca^{2+} and Na^+ to directly increase the $[\text{Ca}^{2+}]_i$ and provides an inwardly directed cation current that could depolarize the sarcolemma and facilitate voltage-dependent Ca^{2+} influx. Blockade of L-type Ca^{2+} channels would not prevent the direct elevation of $[\text{Ca}^{2+}]_i$ by Ca^{2+} entering through ligand-gated channels but could attenuate the maximum peak response by eliminating a voltage-dependent component. Regardless of the mechanisms involved, the current studies demonstrate that Ca^{2+} influx through voltage-gated, L-type Ca^{2+} channels is a primary contributor to the ATP-mediated increase in $[\text{Ca}^{2+}]_i$. Furthermore, there appears to be one or more alternative Ca^{2+} influx pathways that remain to be identified.

The current studies have revealed that ATP stimulates the release of Ca^{2+} from intracellular stores in renal MVSMC in addition to stimulating Ca^{2+} influx. This conclusion is based on the rapid but transient increase in $[\text{Ca}^{2+}]_i$ observed when Ca^{2+} is removed from the extracellular bathing medium. ATP-mediated activation of P2Y receptors has been shown to activate phospholipase C with the subsequent generation of inositol 1,4,5-trisphosphate (IP_3) (1, 9, 10). Previous studies from our laboratory have shown that ATP stimulates both Ca^{2+} influx and Ca^{2+} mobilization in cultured rat renal arterial smooth muscle cells (15). In addition, other investigators have reported that ATP stimulates IP_3 -mediated Ca^{2+} release from intracellular stores in aortic smooth muscle cells, endothelial cells, mesangial cells, and cell lines established from renal epithelium (see Refs. 1, 9, 10, and 26 for review). Therefore, it is reasonable to postulate that ATP-mediated Ca^{2+} mobilization in MVSMC involves activation of phospholipase C.

The physiological significance of P2 receptors in renal microvascular function remains to be established; however, there are interesting data that suggest that P2 receptors may be critically involved in renal hemodynamic control (18, 26). Autoregulatory responses to increases in renal perfusion pressure are largely determined by alterations in preglomerular microvascular resistance. These Ca^{2+} -dependent, pressure-mediated adjustments in preglomerular resistance utilize both Ca^{2+} mobilization and activation of voltage-gated Ca^{2+} channels to regulate active tension in the smooth muscle of the vascular wall (16, 26). Recently, we have postulated that extracellular ATP may function as the

“chemical messenger” responsible for transducing hemodynamic stimuli into appropriate autoregulatory responses (18, 26). Like autoregulatory responses, afferent arteriolar responses to ATP involve voltage-dependent Ca^{2+} influx that can be substantially blocked by Ca^{2+} channel antagonists. In addition, the results of the current study establish that ATP stimulates the release of Ca^{2+} from intracellular stores. These observations demonstrate the essential role Ca^{2+} plays in the preglomerular response to ATP and are consistent with the involvement of P2 receptors in the Ca^{2+} -dependent regulation of renal microvascular resistance and in autoregulatory adjustments in afferent arteriolar diameter.

In summary, the data presented indicate that ATP-mediated P2 receptor activation increases $[\text{Ca}^{2+}]_i$ in freshly isolated preglomerular MVSMC by stimulating Ca^{2+} release from intracellular stores in addition to stimulating the influx of extracellular Ca^{2+} through voltage-gated L-type Ca^{2+} channels.

The authors thank Elizabeth A. LeBlanc and Bao Thang Pham for excellent technical assistance.

This work was supported by American Heart Association Grants AHA-95001370 and AHA-95009790 and by National Institutes of Health Grants DK-44628 and DK-38226. E. W. Inscho is an Established Investigator of the American Heart Association.

Address for reprint requests and other correspondence: E. W. Inscho, Dept. of Physiology SL#39, Tulane Univ. School of Medicine, 1430 Tulane Ave., New Orleans, LA 70112 (E-mail: einscho@mailhost.tcs.tulane.edu).

Received 19 August 1998; accepted in final form 13 November 1998.

REFERENCES

1. **Abbracchio, M. P., and G. Burnstock.** Purinoceptors: are there families of P2X and P2Y purinoceptors? *Pharmacol. Ther.* 64: 445–475, 1994.
2. **Benham, C. D., T. B. Bolton, N. G. Byrne, and W. A. Large.** Action of externally applied adenosine triphosphate on single smooth muscle cells dispersed from rabbit ear artery. *J. Physiol. (Lond.)* 387: 473–488, 1987.
3. **Burnstock, G.** A basis for distinguishing two types of purinergic receptor. In: *Cell Membrane Receptors for Drugs and Hormones: A Multidisciplinary Approach*, edited by L. Bolis and R. C. O. Straub. New York: Raven, 1978, p. 107–118.
4. **Carmines, P. K., B. C. Fowler, and P. D. Bell.** Segmentally distinct effects of depolarization on intracellular $[\text{Ca}^{2+}]_i$ in renal arterioles. *Am. J. Physiol.* 265 (*Renal Fluid Electrolyte Physiol.* 34): F677–F685, 1993.
5. **Carmines, P. K., and L. G. Navar.** Disparate effects of Ca channel blockade on afferent and efferent arteriolar responses to ANG II. *Am. J. Physiol.* 256 (*Renal Fluid Electrolyte Physiol.* 25): F1015–F1020, 1989.
6. **Casellas, D., and P. K. Carmines.** Control of the renal microcirculation: cellular and integrative perspectives. *Curr. Opin. Nephrol. Hypertens.* 5: 57–63, 1996.
7. **Chan, C. M., R. J. Unwin, M. Bardini, I. B. Oglesby, A. P. Ford, A. Townsend-Nicholson, and G. Burnstock.** Localization of the P2X₁ purinoceptors by autoradiography and immunohistochemistry in rat kidneys. *Am. J. Physiol.* 274 (*Renal Physiol.* 43): F799–F804, 1998.
8. **Conger, J. D., and S. A. Falk.** KCl and angiotensin responses in isolated rat renal arterioles: effects of diltiazem and low-calcium medium. *Am. J. Physiol.* 264 (*Renal Fluid Electrolyte Physiol.* 33): F134–F140, 1993.
9. **Dubyak, G. R., and C. El-Moatassim.** Signal transduction via P2-purinergic receptors for extracellular ATP and other nucleotides. *Am. J. Physiol.* 265 (*Cell Physiol.* 34): C577–C606, 1993.
10. **El-Moatassim, C., J. Dornand, and J.-C. Mani.** Extracellular ATP and cell signaling. *Biochim. Biophys. Acta* 1134: 31–45, 1992.

11. **Fredholm, B. B., M. P. Abbracchio, G. Burnstock, J. W. Daly, T. K. Harden, K. A. Jacobson, P. Leff, and M. Williams.** Nomenclature and classification of purinoceptors. *Pharmacol. Rev.* 46: 143–156, 1994.
12. **Gordienko, D. V., C. Clausen, and M. S. Goligorsky.** Ionic currents and endothelin signaling in smooth muscle cells from rat resistance arteries. *Am. J. Physiol.* 266 (*Renal Fluid Electrolyte Physiol.* 35): F325–F341, 1994.
13. **Gryniewicz, G., M. Poenie, and R. Y. Tsien.** A new generation of calcium indicators with greatly improved fluorescence properties. *J. Biol. Chem.* 260: 3440–3450, 1985.
14. **Hayashi, K., M. Epstein, and R. Loutzenhiser.** Pressure-induced vasoconstriction of renal microvessels in normotensive and hypertensive rats: studies in the isolated perfused hydronephrotic kidney. *Circ. Res.* 65: 1475–1484, 1989.
15. **Inscho, E. W., T. P. Belott, M. J. Mason, J. B. Smith, and L. G. Navar.** Extracellular ATP increases cytosolic calcium in cultured renal arterial smooth muscle cells. *Clin. Exp. Pharmacol. Physiol.* 23: 503–507, 1996.
16. **Inscho, E. W., A. K. Cook, V. Mui, and J. D. Imig.** Calcium mobilization contributes to pressure-mediated afferent arteriolar vasoconstriction. *Hypertension* 31: 421–428, 1998.
17. **Inscho, E. W., A. K. Cook, V. Mui, and J. Miller.** Direct assessment of renal microvascular responses to P2-purinoceptor agonists. *Am. J. Physiol.* 274 (*Renal Physiol.* 43): F718–F727, 1998.
18. **Inscho, E. W., A. K. Cook, and L. G. Navar.** Pressure-mediated vasoconstriction of juxtamedullary afferent arterioles involves P2-purinoceptor activation. *Am. J. Physiol.* 271 (*Renal Fluid Electrolyte Physiol.* 40): F1077–F1085, 1996.
19. **Inscho, E. W., M. J. Mason, A. C. Schroeder, P. C. Deichmann, K. D. Steigler, and J. D. Imig.** Agonist-induced calcium regulation in freshly isolated renal microvascular smooth muscle cells. *J. Am. Soc. Nephrol.* 8: 569–579, 1997.
20. **Inscho, E. W., K. Ohishi, A. K. Cook, T. P. Belott, and L. G. Navar.** Calcium activation mechanisms in the renal microvascular response to extracellular ATP. *Am. J. Physiol.* 268 (*Renal Fluid Electrolyte Physiol.* 37): F876–F884, 1995.
21. **Inscho, E. W., K. Ohishi, and L. G. Navar.** Effects of ATP on pre- and postglomerular juxtamedullary microvasculature. *Am. J. Physiol.* 263 (*Renal Fluid Electrolyte Physiol.* 32): F886–F893, 1992.
22. **Kitajima, S., H. Ozaki, and H. Karaki.** Role of different subtypes of P2 purinoceptor on cytosolic Ca^{2+} levels in rat aortic smooth muscle. *Eur. J. Pharmacol.* 266: 263–267, 1994.
23. **Loutzenhiser, R., L. Chilton, and G. Trottier.** Membrane potential measurements in renal afferent and efferent arterioles: actions of angiotensin II. *Am. J. Physiol.* 273 (*Renal Physiol.* 42): F307–F314, 1997.
24. **Loutzenhiser, R., and M. Epstein.** Renal microvascular actions of calcium antagonists. *J. Am. Soc. Nephrol.* 1: S3–S12, 1990.
25. **Mitchell, K. D., and L. G. Navar.** Tubuloglomerular feedback responses during peritubular infusions of calcium channel blockers. *Am. J. Physiol.* 258 (*Renal Fluid Electrolyte Physiol.* 27): F537–F544, 1990.
26. **Navar, L. G., E. W. Inscho, D. S. A. Majid, J. D. Imig, L. M. Harrison-Bernard, and K. D. Mitchell.** Paracrine regulation of the renal microcirculation. *Physiol. Rev.* 76: 425–536, 1996.
27. **Rembold, C. M., B. A. Weaver, and J. Linden.** Adenosine triphosphate induces a low $[Ca^{2+}]_i$ sensitivity of phosphorylation and an unusual form of receptor desensitization in smooth muscle. *J. Biol. Chem.* 266: 5407–5411, 1991.
28. **Soto, F., M. Garcia-Guzman, and W. Stühmer.** Cloned ligand-gated channels activated by extracellular ATP (P2X receptors). *J. Membr. Biol.* 160: 91–100, 1997.
29. **Steinhausen, M., and M. Baehr.** Vasomotion and vasoconstriction induced by a Ca^{2+} agonist in the split hydronephrotic kidney. *Prog. Appl. Microcirc.* 14: 25–39, 1989.
30. **Strobaek, D., P. Christophersen, S. Dissing, and S. P. Olesen.** ATP activates K and Cl channels via purinoceptor-mediated release of Ca^{2+} in human coronary artery smooth muscle. *Am. J. Physiol.* 271 (*Cell Physiol.* 40): C1463–C1471, 1996.
31. **Takenaka, T., H. Suzuki, K. Fujiwara, Y. Kanno, Y. Ohno, K. Hayashi, T. Nagahama, and T. Saruta.** Cellular mechanisms mediating rat renal microvascular constriction by angiotensin II. *J. Clin. Invest.* 100: 2107–2114, 1997.
32. **Tawada, Y., K. Furukawa, and M. Shigekawa.** ATP-induced transient in cultured rat aortic smooth muscle cells. *J. Biochem. (Tokyo)* 102: 1499–1509, 1987.
33. **Von der Weid, P., V. N. Serebryakov, F. Orallo, C. Bergmann, V. A. Snetkov, and K. Takeda.** Effects of ATP on cultured smooth muscle cells from the rat aorta. *Br. J. Pharmacol.* 108: 638–645, 1993.
34. **Wagner, A. J., N. Holstein-Rathlou, and D. J. Marsh.** Endothelial Ca^{2+} in afferent arterioles during myogenic activity. *Am. J. Physiol.* 270 (*Renal Fluid Electrolyte Physiol.* 39): F170–F178, 1996.
35. **Weihprecht, H., J. N. Lorenz, J. P. Briggs, and J. Schnermann.** Vasomotor effects of purinergic agonists in isolated rabbit afferent arterioles. *Am. J. Physiol.* 263 (*Renal Fluid Electrolyte Physiol.* 32): F1026–F1033, 1992.